available at www.sciencedirect.com

ScienceDirect

www.elsevier.com/locate/brainres

BRAIN RESEARCH

Research Report

Cellular responses in the spinal cord during development of hypomyelination in the *mv* rat

Takeshi Izawa[a], *Shigeo Takenaka*[a], *Hideshi Ihara*[b], *Takao Kotani*[a], *Jyoji Yamate*[a], *Robin J.M. Franklin*[c], *Mitsuru Kuwamura*[a,*]

[a]*Department of Veterinary Sciences, Osaka Prefecture University, Gakuencho 1-1, Nakaku, Sakai, Osaka 599-8531, Japan*
[b]*Department of Biological Science, Osaka Prefecture University, Gakuencho 1-1, Nakaku, Sakai, Osaka 599-8531, Japan*
[c]*Department of Veterinary Medicine and Cambridge Centre for Brain Repair, University of Cambridge, Madingley Road, Cambridge, CB3 0ES, UK*

ARTICLE INFO

Article history:
Accepted 12 December 2007
Available online 23 December 2007

Keywords:
Attractin
Hypomyelination
Astrogliosis
Microglial activation

ABSTRACT

The myelin vacuolation (*mv*) rat is an autosomal recessive mutant characterized by hypomyelination and vacuole formation in the myelin throughout the central nervous system (CNS). Previous genetic studies have revealed a null mutation in attractin gene of the *mv* mutant rat. It has been known that mutation at the attractin locus results in myelin alterations, but their detailed pathogenesis is still unclear. In this study, we examined glial changes in the spinal cord of *mv* rats at 2, 4, 6, and 8 weeks of age and identified attractin-expressing cells in the rat spinal cord. No abnormality was found in the number and morphology of oligodendrocytes in *mv* rats at any of the ages examined, although the severity and extent of myelin disorder increased with age. Coincident with the myelin abnormalities, there was progressive astrogliosis from 2 weeks. Marked microglial activation was observed exclusively in the gray matter of *mv* rats from 6 weeks, coincident with severe myelin disruption. A double-labeling study demonstrated that attractin-expressing cells are mostly oligodendrocytes in the white matter of the spinal cord of wild-type rats, whereas no attractin-positive cells were detected in *mv* rats. Previous study demonstrated that Luxol fast blue staining pattern and immunoreactivity for myelin basic protein were decreased in *mv* rats. Therefore, this study indicates that the attractin defect results in oligodendrocyte dysfunction, and is associated with astrogliosis and microglial activation in *mv* rats. The data suggest that attractin may be directly involved in the function of oligodendrocytes in CNS myelination.

* *Corresponding author*. Fax: +81 72 250 7208.
E-mail address: kuwamura@vet.osakafu-u.ac.jp (M. Kuwamura).

Abbreviations: EGF, epidermal growth factor; CNS, central nervous system; PLP, proteolipid protein; GFAP, glial fibrillary acidic protein; PCR, polymerase chain reaction; PFA, paraformaldehyde; PB, phosphate buffer; PBS, phosphate-buffered saline; CNPase, 2′, 3′-cyclic nucleotide-3′-phosphodiesterase; RT-PCR, reverse transcriptase polymerase chain reaction; TNF, tumor necrosis factor; IL, interleukin; iNOS, inducible nitric oxide synthase; TGF, transforming growth factor; Ct, threshold cycle; SSC, sodium saline citrate; FITC, fluorescein isothiocyanate; NO, nitric oxide; MS, multiple sclerosis; EAE, experimental autoimmune encephalomyelitis

0006-8993/$ – see front matter © 2008 Elsevier B.V. All rights reserved.
doi:10.1016/j.brainres.2007.12.022

1. Introduction

Attractin (ATRN) is a glycoprotein initially found in human activated T cells and consists of a secreted and a membrane isoform as a result of alternative splicing (Duke-Cohan et al., 1995, 1998; Tang et al., 2000). Both isoforms contain a CUB domain, two epidermal growth factor (EGF) domains, a C-type lectin domain, and two laminin-type EGF domains in the extracellular region, suggesting potential roles in cell adhesion, cell–cell interaction, or signaling. The transmembrane orthologue was found as the product of the mouse mahogany gene while no secreted form was identified in mice (Gunn et al., 1999; Nagle et al., 1999). Studies on human immunology and in mahogany mutant mice (*Atrn*^{mg}) have revealed that attractin has multiple functions including T cell-monocyte/macrophage interaction, agouti-related hair pigmentation, and control of energy homeostasis (Dinulescu et al., 1998; Duke-Cohan et al., 1998, 2000; Nagle et al., 1999; He et al., 2001). The mutation at the *Atrn* locus also has been identified in rats (zitter [*Atrn*^{zi}] and myelin vacuolation [*mv*, *Atrn*^{mv}]) (Kuramoto et al., 2001; Kuwamura et al., 2002) and Syrian hamsters (black tremor, *Atrn*^{bt}) (Kuramoto et al., 2002). All of these *Atrn* mutant animals have been characterized by hypomyelination and vacuolation in the central nervous system (CNS) and, in varying degrees, body tremor (Kuramoto et al., 2001, 2002; Kuwamura et al., 2002; Nunoya et al, 1985). Transgenic rescue experiments demonstrated that only membrane-type attractin complemented neurological alteration in the zitter rat, indicating its critical role in normal myelination and myelin maintenance in the CNS (Kuramoto et al., 2001). Thus the *Atrn* mutant animals provide a useful model for studying the role of attractin in CNS myelination.

The *mv* rat is an autosomal recessive mutant found in a colony of Sprague–Dawley rats and exhibits tremor behavior from around 3 weeks of age (Kuwamura et al., 2002). The pathological characters are hypomyelination and vacuolation throughout the CNS, especially in the brain stem, cerebellum, and spinal cord. By electron microscopy, the vacuoles are revealed to consist mainly of splitting between myelin lamellae. Genetic studies revealed a 6.9-kb deletion including the whole exon 1 of the attractin gene in *mv* rats (Tokuda et al., 2004) and Northern blot analysis showed no expression of *Atrn* mRNA in the brain of *mv* rats (Kuwamura et al., 2002). Therefore, the *mv* rat is a null mutant of the *Atrn* gene.

It is well known that mutations at genes encoding myelin protein or genes associated with oligodendroglial function result in abnormalities in myelination and myelin maintenance.

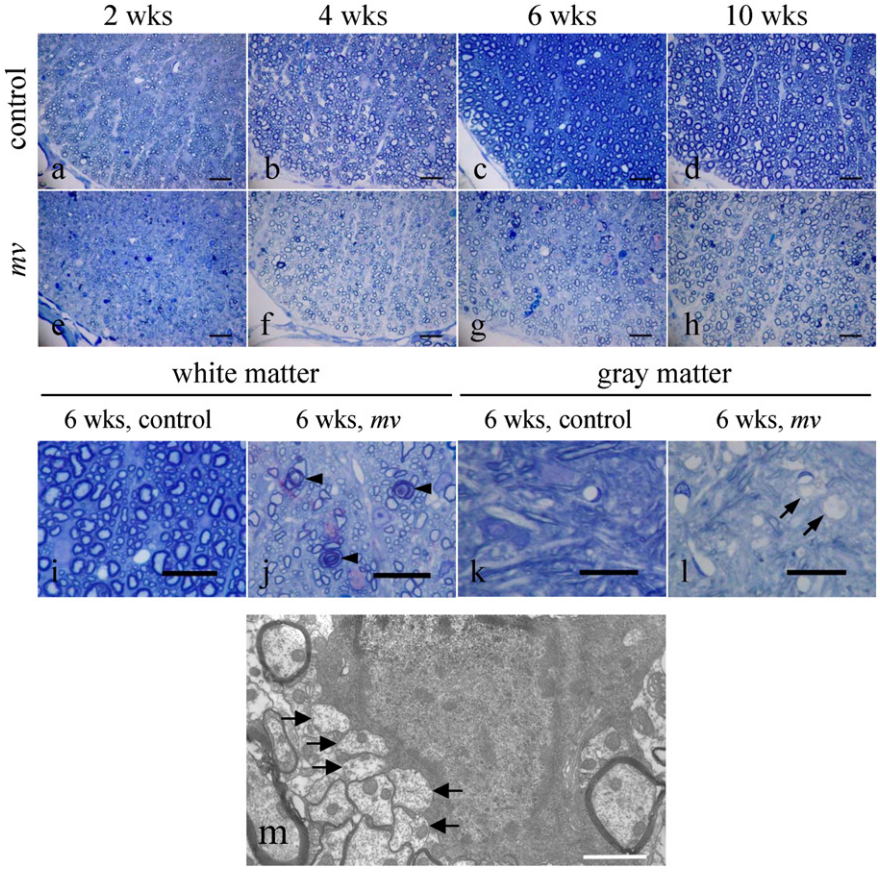

Fig. 1 – Toluidine blue stained sections from the white matter of the lumbar spinal cord in control (a–d) and *mv* (e–h) rats. There are many abnormal myelin sheaths (*arrowheads*) in the white matter of the 6-week-old *mv* rat (j). From 6 weeks, vacuolation (*arrow*) starts to appear in the gray matter of the *mv* rat (l). Electron micrograph of the white matter of the lumbar spinal cord of the 6-week-old *mv* rat (m). There are many unmyelinated or hypomyelinated axons (*arrows*) in the *mv* rat while no ultrastructural abnormality is found in oligodendrocytes. *Bar*: 20 μm (a–l), 1.4 μm (m).

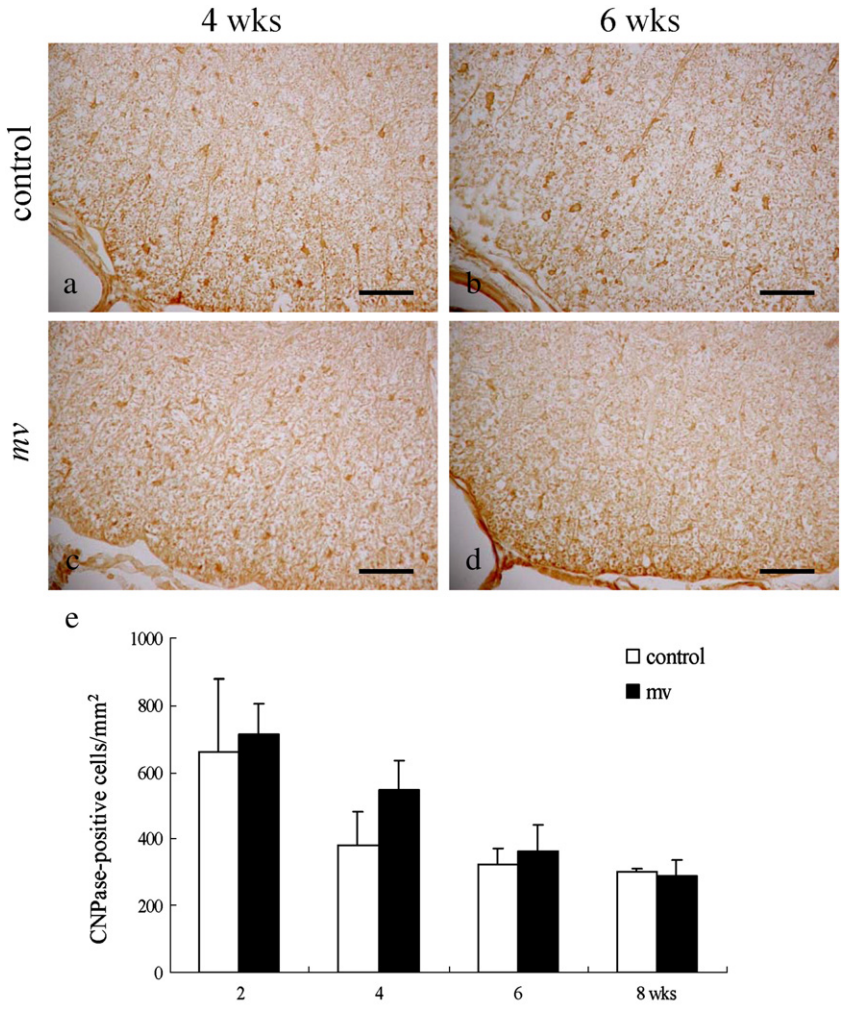

Fig. 2 – CNPase immunohistochemistry in the ventral funiculus of control (a, b) and *mv* (c, d) rats. The graph shows the number of CNPase-positive oligodendrocytes in the dorsal funiculus of the lumbar spinal cord (e). There is no significance between control (*open bars*) and *mv* (*black bars*) rats ($n=3$ in each group) at any of the ages by Scheffe's test. *Bar*: 100 μm.

In the jimpy mouse, having a severe CNS myelin deficit with a X-linked mutation in the proteolipid protein (PLP)/DM20 gene, the numbers of mature oligodendrocytes are severely reduced (Skoff, 1976) and this is explained by the premature cell death of oligodendrocytes (Knapp et al., 1986). In the Long Evans Shaker (*les*) rat, a dysmyelinating mutant with an insertional

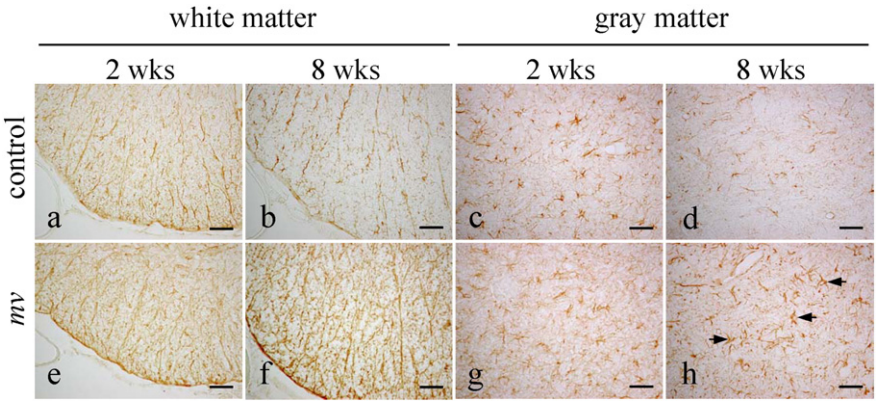

Fig. 3 – GFAP immunohistochemistry in control (a–d) and *mv* (e–h) rats. Increased GFAP immunoreactivity is observed in the white matter of *mv* rats from 2 weeks (e). Hypertrophic astrocytes (*arrows*) are found in the gray matter of the 8-week-old *mv* rats (h). *Bar*: 40 μm.

mutation in the myelin basic protein gene (Delaney et al., 1995; O'Connor et al., 1999), the numbers of mature oligodendrocytes are similar to controls early in life and increase with age, although CNS myelin is gradually lost, indicating an inability of oligodendrocytes to maintain myelin (Kwiecien et al., 1998). The taiep rat exhibits progressive neurological symptom (tremor, ataxia, immobility, epilepsy, paralysis) (Holmgren et al., 1989) and is characterized by early hypomyelination and subsequent demyelination (Duncan et al., 1992; Lunn et al., 1997). In taiep rats, microtubule abnormalities are found in oligodendrocytes from the time of onset of myelination (Lunn et al., 1997), which is directly associated with the myelin deficit (Song et al., 1999). Besides oligodendrocyte alterations, changes in astrocytes and microglia are commonly observed in these myelin mutants. Jimpy mutant mice show a striking hypertrophy of astrocytic process and increased immunoreactivity of glial fibrillary acidic protein (GFAP) (Omlin and Anders, 1983; Skoff, 1976), and an intense microglial cell reaction that is more pronounced in the white matter than in the gray matter and considered to be related to apoptotic oligodendrocytes (Vela et al., 1995, 1996). In *les* rats, progressive astrocytic hypertrophy and microgliosis are localized to the white matter (Kwiecien et al., 1998; Zhang et al., 2001). In taiep rats, progressive reactive astrocytosis is developed in the brain regions where hypomyelination is more severe (Leon Chavez et al., 2001), and the number of OX-42 positive microglia/macrophages is increased in the cerebellar white matter (Leon Chavez et al., 2006). The pattern and degree of glial abnormalities vary in each mutant, but are tightly associated with myelin lesions, in terms of both location and time course.

Here we describe the identification of *Atrn*-expressing cells in the rat CNS by double-labeling method and examine

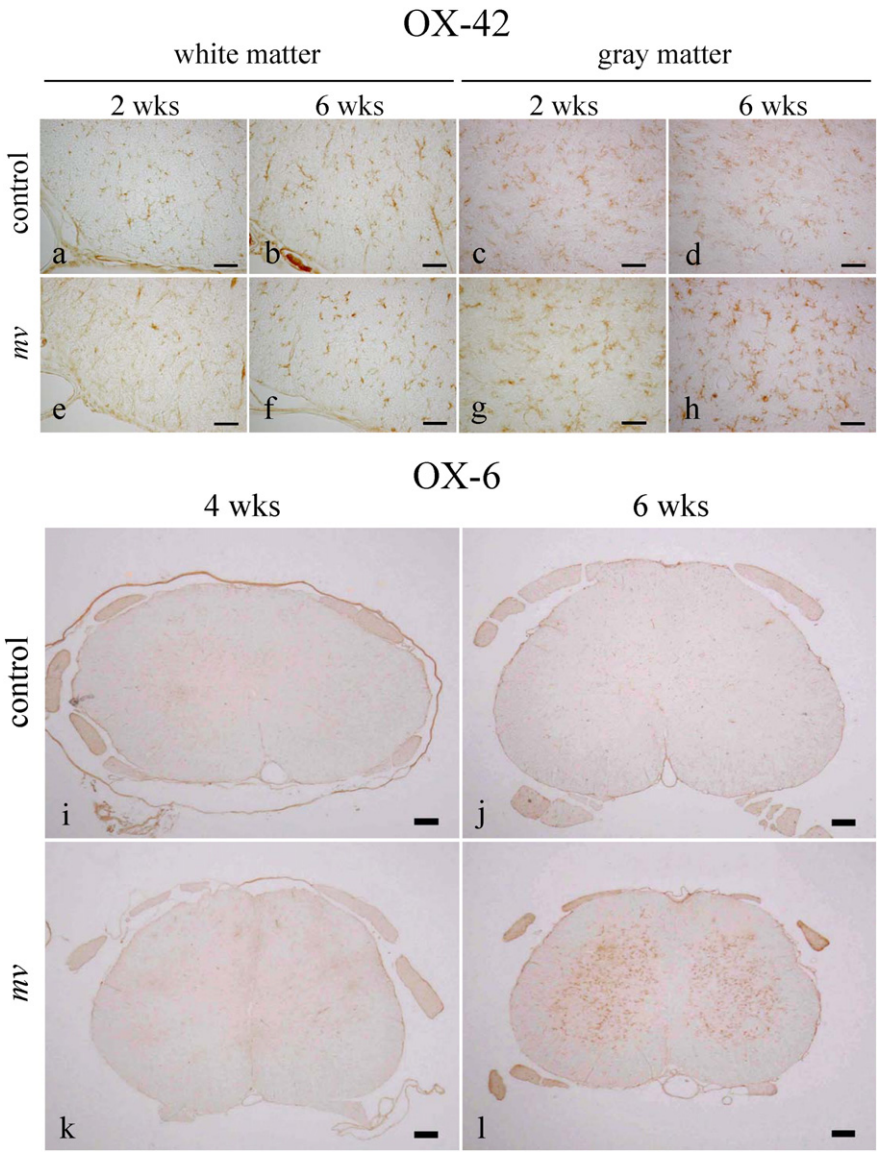

Fig. 4 – Immunohistochemistry for OX-42 (a–h) and OX-6 (i–l). There are many activated microglia with swollen cell bodies and shortened processes in the gray matter of *mv* rats from 6 weeks (h), while no apparent change in microglial morphology is observed in the white matter of *mv* rats at any of the ages (e, f). OX-6 immunostaining shows that microglial activation in *mv* rats from 6 weeks is exclusively found in the gray matter (l). *Bar*: 40 μm (a–h), 200 μm (i–l).

astrocyte and microglia changes in the spinal cord of the *mv* rat during the evolution of the pathological phenotype. Our results show that *Atrn*-expressing cells are mainly oligodendrocytes in the spinal cord white matter of wild-type rats and that a progressive astrogliosis begins from an early age in *mv* rats followed by marked microglial activation occurring predominantly in the gray matter when the myelin lesions are most severe. Our results suggest a direct role for attractin in the CNS myelination.

2. Results

2.1. *Myelin abnormalities increase within spinal cord white and gray matter during post-natal development*

To understand the progression of myelin pathology in the *mv* rat, we first examined temporal changes in the spinal cord. At 2 weeks, fewer myelinated axons and thinner myelin sheaths were found in the white matter of *mv* rats compared with age-matched controls (Fig. 1a, e). This hypomyelination became more prominent with age (Fig. 1). Also present in the *mv* rat were variously-sized vacuoles and abnormal myelin sheaths, which were due to splitting of myelin sheaths as previously described (Kuwamura et al., 2002). From 6 weeks, these aberrant myelin structures were frequently observed in the white matter (Fig. 1i–j; indicated by arrowheads) and vacuolation extended into the gray matter (Fig. 1k–l; indicated by arrows). In electron microscopy, naked or hypomyelinated axons were observed in the *mv* rat (Fig. 1m; indicated by arrows), while no obvious ultrastructural abnormality was found in oligodendrocytes (Fig. 1m).

2.2. *Myelin pathology is associated with increased astrogliosis but no changes in oligodendrocyte numbers or morphology, while microglial activation is mainly confined to the gray matter*

We next investigated cellular changes in the *mv* rat by immunohistochemistry with specific glial markers. There were no prominent changes in the distribution and morphology of CNPase-positive oligodendrocytes between control and *mv* rats at any of the ages examined (Fig. 2a–d), neither did the number of CNPase-positive oligodendrocytes differ significantly, although their density gradually reduced with age in both groups (Fig. 2e). Compared to control rats, GFAP immunoreactivity in the white matter of the spinal cord was increased in *mv* rats from 2 weeks (Fig. 3a, e), and was more pronounced at 8 weeks (Fig. 3b, f). In the gray matter, the morphology of astrocytes was similar in both control and *mv* rats at 2 weeks (Fig. 3c, g), but from 6 weeks, the astrocytes in *mv* rats showed hypertrophy of their processes, a common feature of activated astrocytes (Fig. 3h; arrows). OX-42 immunohistochemistry was used to detect microglia in control and *mv* rats (Fig. 4a–h). Microglial morphology in the white matter of *mv* rats was almost similar to controls at all ages (Fig. 4a, b, e, f). In the gray matter, the morphology of microglia was not prominently changed in either control or *mv* rats up to 4 weeks (Fig. 4c, g), but from 6 weeks, the microglia in *mv* rats had an activated morphology, characterized by swollen cell bodies and shortened processes (Fig. 4d, h). Furthermore, OX-6

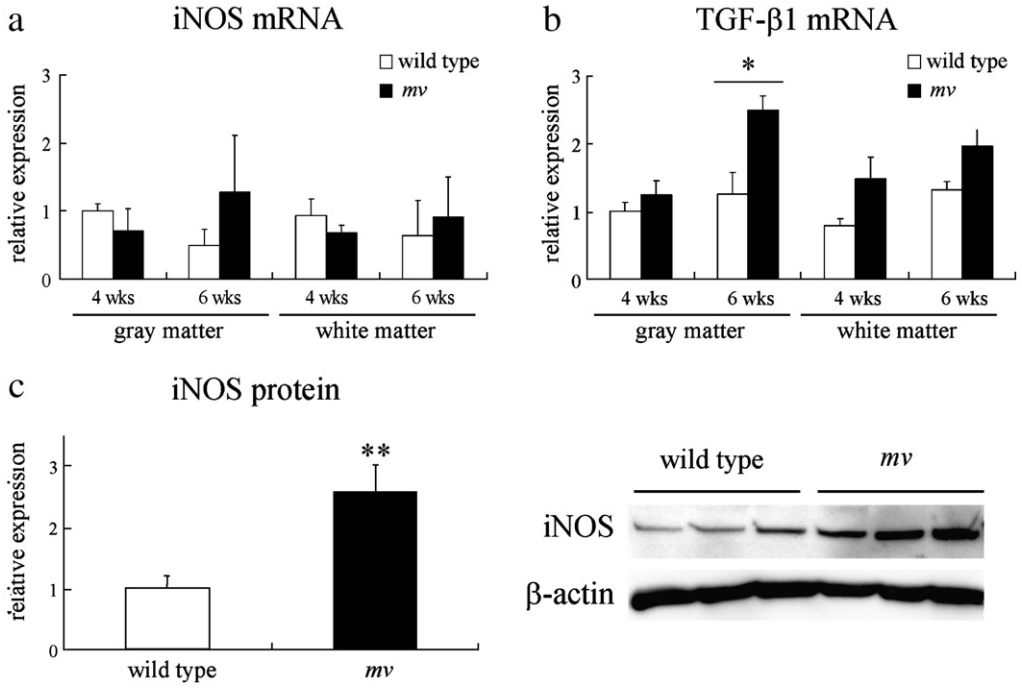

Fig. 5 – Expression levels of iNOS (a) and TGF-β1 (b) gene. Each data represents relative expression level to β-actin ($n=3$ in each group). * $P<0.01$, compared to wild-type rats. Expression level of iNOS protein from the spinal cord of wild-type and *mv* rats at 10 weeks (c). Data are presented as relative expression level normalized by that of β-actin. Compared to wild-type rats, expression level of iNOS protein is significantly increased in *mv* rats. ** $P<0.01$, compared to wild-type rats.

immunohistochemistry revealed microglial activation in *mv* rats from 6 weeks, which was exclusively found in the gray matter (Fig. 4i–l).

2.3. *Microglial activation is associated with increases in iNOS expression and TGF-β1*

To gain further insights into the properties of the activated microglia in the *mv* rat, we examined expression levels of several factors associated with activated microglia in human and animal myelin diseases (Zhang et al., 2001; Leon Chavez et al., 2006; Raivich and Banati, 2004). Expression level of the iNOS gene in gray matter of *mv* rats at 6 weeks was slightly elevated compared to the levels in wild-type rats (Fig. 5a). Western blot analysis demonstrated significantly increased expression of iNOS protein in the spinal cord of *mv* rats at 10 weeks (Fig. 5c). There was no obvious difference in protein expression level of β-actin between wild-type and *mv* rats. Expression level of TGF-β1 gene was significantly higher in the gray matter of *mv* rats than in wild-type rats at 6 weeks (Fig. 5b). There were no obvious changes in expression levels of TNF-α, IL-1β, and IL-6 gene between wild-type and *mv* rats at 4 and 6 weeks (data not shown).

2.4. *Atrn mRNA is mainly expressed by CNPase-positive oligodendrocytes in the white matter*

We used double-labeling by *in situ* hybridization and immunohistochemistry to identify *Atrn*-expressing cells in the rat CNS. *Atrn*-positive cells were widely distributed both in the white (Fig. 6a) and gray (Fig. 6d) matter of wild-type spinal cords, while no signal was detected in the spinal cord of *mv* rats (Fig. 6h). No specific signal was found in either wild-type or *mv* rats when an *Atrn* sense probe was used (data not shown). *Atrn* mRNA was expressed mostly in CNPase-positive oligodendrocytes in the white matter (Fig. 6a–c; arrowheads). In the gray matter, GFAP-positive astrocytes were also positive for *Atrn* (Fig. 6d–f; arrow). *Atrn*-positive cells were also occasionally found in the gray matter, which were morphologically suggestive of neurons, due to their abundant cytoplasm and large nuclei (Fig. 6g).

3. Discussion

In the *mv* rat, hypomyelination and abnormal myelination were observed in the white matter of the spinal cord from 2 weeks, the severity of which progressed with age. Despite progressive myelin pathology, the number and morphology of oligodendrocytes in *mv* rats were almost similar to those in controls at all ages examined. In jimpy mice, oligodendrocytes proliferate but die rapidly through apoptosis (Knapp et al., 1986), which may result from the accumulation of misfolded PLP in the endoplasmic reticulum (Gow et al., 1994). The *les* rat shows abnormal accumulation of vesicular organelles in the cytoplasm of oligodendrocytes, which may reflect a failure of myelin production and formation (Kwiecien et al., 1998). In the taiep rat, the myelin deficit has been directly associated with microtubule alterations in oligodendrocytes (Song et al, 1999), and with alterations in expression and intracellular distribution of myelin gene products (O'Connor et al., 2000). In the *mv* rat, no degenerating oligodendrocytes were seen under light microscope, and no ultrastructural abnormality in oligodendrocytes was observed. Our results show that oligodendrocytes in the *mv*

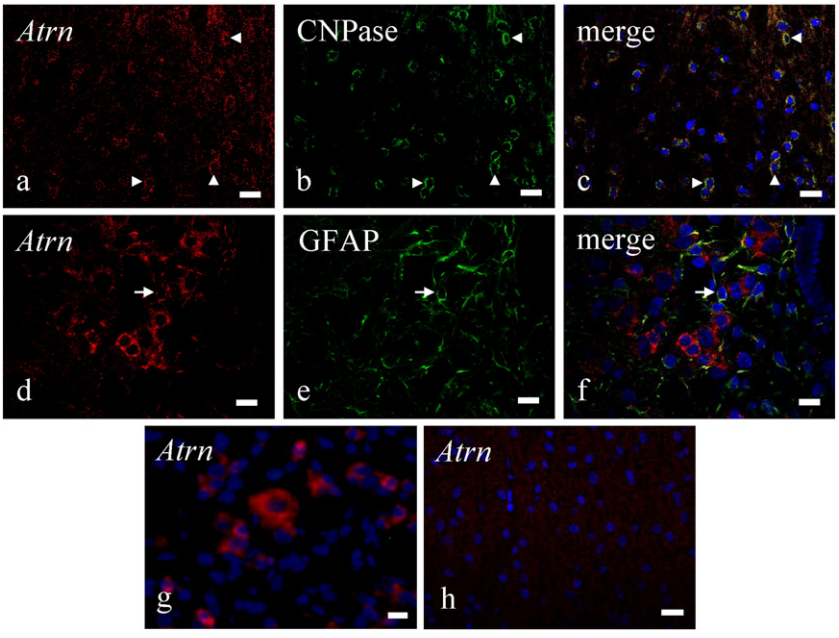

Fig. 6 – Identification of *Atrn* mRNA-expressing cells. *Atrn in situ* hybridization and CNPase immunohistochemistry in the white matter of the wild-type rat (a–c). *Atrn in situ* hybridization and GFAP immunohistochemistry in the gray matter of the wild-type rat (d–f). In the gray matter, neurons are occasionally positive for *Atrn in situ* hybridization (g). No specific signal is detected in the *mv* rat by *Atrn in situ* hybridization (h). Red; *Atrn in situ* hybridization, green; immunohistochemistry (FITC), blue; nuclei (DAPI). *Arrowheads*; $Atrn^+$/$CNPase^+$ cells, *Arrow*; $Atrn^+$/$GFAP^+$ cells. *Bar*: 20 μm.

rat do not undergo direct cell injury or death, but have some dysfunction in formation and maintenance of CNS myelin.

In situ hybridization combined with immunolabeling revealed that *Atrn* mRNA-expressing cells were mostly oligodendrocytes in the spinal cord white matter of wild-type rats, and that no *Atrn*-positive signals were detected in the *mv* rat. These results suggest that the membrane-type attractin is involved in oligodendrocyte function. Recently, a biochemical study showed the progressive loss of lipid-raft domains and reduction in cellular cholesterol in *Atrn*-deficient mice, proposing that the juvenile-onset hypomyelination and neurodegeneration represent a defect in attractin-mediated raft-dependent myelin biogenesis (Azouz et al., 2007). Lipid rafts are detergent-insoluble glycolipid-enriched membrane microdomains that participate in protein sorting and trafficking (Simons and Ikonen, 1997) and may take a critical role in forming the myelin membrane (Simons et al., 2000). Together with these findings, our results show that attractin is likely to be directly involved in the function of oligodendrocytes in CNS myelination. Precise pathogenesis for hypomyelination in *mv* rats remains to be elucidated. It would be necessary to carry out detailed studies on function of oligodendrocyte and on the relationship between oligodendrocytes and axons in *Atrn*-deficient animals.

We found increased GFAP immunoreactivity in the white matter of the spinal cord in *mv* rats from 2 weeks, which progressed with age. Hypertrophic astrocytes also appeared in the gray matter of *mv* rats from 6 weeks. The regional and temporal pattern of astrocyte alterations accorded with that of myelin lesions in the *mv* rat, and these astrocytic changes are commonly observed in myelin mutants. In *les* rats, the temporal pattern of astrocyte hypertrophy corresponds to that of defective myelination and the distribution of reactive astrocytes is dominant in the white matter, indicating an astrocyte response to the white matter lesion (Zhang et al., 2001). Similarly, the progressive astrogliosis is considered as a reactive change in taiep rats, due to its regional and temporal pattern that correlates with the process of dysmyelination (Leon Chavez et al., 2001). Unlike *les* and taiep rats, astrocyte abnormalities in jimpy mice are observed not only during myelination but also in early post-natal development, before mature oligodendrocytes appear, supporting but not proving a causative effect of astrocytes on myelin deficit (Omlin and Anders, 1983; Skoff, 1976). Our results suggest that progressive astrogliosis is closely associated with myelin pathology in the *mv* rat, but further study is needed to determine whether astrocyte alterations of the *mv* rat are causative or reactive.

OX-42 and OX-6 immunohistochemistry demonstrated numerous activated microglia in the gray matter of the spinal cord in *mv* rats from 6 weeks. The onset time of microglial activation coincided with the progression of myelin pathology. However, the distribution of activated microglia did not correlate with the myelin lesions that were predominant in the white matter. This distribution was clearly different from other myelin mutants such as jimpy mice (Vela et al., 1995, 1996), *les* rats (Zhang et al., 2001), and taiep rats (Leon Chavez et al., 2006), where the microglial reaction is limited to the white matter. In addition, we did not observe any phagocytic microglia or degenerating neurons in *mv* rats at any age examined. Thus, it is not likely that activation of microglia in this mutant is a mere reaction to myelin disruption or neural degeneration. In the *mv* rat, expression level of iNOS gene was slightly increased in the gray matter of the spinal cord at 6 weeks, and iNOS protein was upregulated in the spinal cord at 10 weeks. Nitric oxide (NO) and its reactant with superoxide, peroxynitrite have been known as toxic factors for oligodendrocytes (Boullerne and Benjamins, 2006; Smith et al., 1999) and mediators of damage to myelin (Bizzozero et al., 2004; Boullerne and Benjamins, 2006; Smith et al., 1999; van der Veen and Roberts, 1999), and their increased production has been reported in multiple sclerosis (MS) (Smith et al., 1999) and in experimental autoimmune encephalomyelitis (EAE), an animal model of MS (Raivich and Banati, 2004). In the demyelinating lesions of MS and EAE, iNOS is induced in various cell types, mainly reactive microglia/macrophages and astrocytes (Hill et al., 2004; Liu et al., 2001; Raivich and Banati, 2004). Although the cell types expressing iNOS have not been identified in the *mv* rat, our results suggest that increased expression of iNOS is at least accompanied by microglial and astrocyte activation found in the *mv* rat, and that activated microglia and/or astrocytes are possible source of iNOS in the spinal cord lesions of the *mv* rat. Besides iNOS, the expression level of TGF-β1 gene was significantly increased in the gray matter of the spinal cord in *mv* rats at 6 weeks, which correlated both temporally and regionally with microglial activation. TGF-β1 is normally present at low levels in the normal CNS tissues, whereas, in many neurodegenerative diseases, it is highly upregulated in various cell types, such as activated microglia and astrocytes, and neurons (Finch et al., 1993; Kiefer et al., 1998; Vivien and Ali, 2006; Zhu et al., 2000). A study in TGF-β1-deficient mice revealed a role in regulating microglial activation (Brionne et al., 2003), and *in vitro* studies demonstrated that TGF-β1 regulates microglial activity by inhibiting iNOS expression (Lieb et al., 2003; Vincent et al., 1997) and NO production (Herrena-Molina and von Bernhardi, 2005; Lieb et al., 2003). In agreement with these findings, our results show that enhanced expression of TGF-β1 gene is closely linked to microglial activation in the *mv* rat. Further study is required to determine why microglial activation is limited to gray matter and how it is involved in myelin pathology in the *mv* rat.

In the *mv* rat, absence of attractin in oligodendrocytes is associated with severe hypomyelination and impaired myelin maintenance in the CNS. Although the exact function of attractin in CNS myelination remains unclear, it suggests that attractin may play a direct role in oligodendrocyte myelination. Thus, attractin mutant animals may serve as a useful model for studying oligodendrocyte function in CNS myelination.

4. Experimental procedures

4.1. *Animals*

Rats were bred and maintained in a mixed Sprague–Dawley/Donryu background in our laboratory. Homozygous *mv* (*mv*/*mv*) rats were obtained by mating heterozygous (*mv*/+) females with heterozygous males. The genotype of each rat was determined by polymerase chain reaction (PCR) using diagnostic primer sets (Tokuda et al., 2004). Rats were maintained in a room with controlled temperature and 12-h light–dark cycle. Food and

water were provided *ad libitum*. Rats were handled according to the Guidelines for Animal Experimentation of Osaka Prefecture University.

4.2. Histology and immunohistochemistry

For morphological analysis, control (+/+ or *mv*/+) and *mv* homozygous rats at 2, 4, 6, and 10 weeks of age were deeply anesthetized with diethylether and perfused transcardially with 4% paraformaldehyde (PFA) in 0.1 M phosphate buffer (PB; pH 7.4). Removed lumbar spinal cords were stored in 2% PFA and 2.5% glutaraldehyde in 0.1 M PB, postfixed with 2% osmic acid for 2 h, and embedded in epoxy resin. One μm semi-thin sections were cut and stained with toluidine blue. Ultrathin sections were stained with uranyl acetate and lead citrate and examined in a Hitachi H-7500 electron microscope (Hitachi, Tokyo, Japan). For immunohistochemistry, control and *mv* rats at 2, 4, 6, and 8 weeks of age were perfused transcardially with 4% PFA in 0.1 M PB. Spinal cords were then removed and postfixed in 4% PFA in 0.1 M PB at 4 °C overnight. After 2- or 3-day treatment with 30% sucrose in phosphate-buffered saline (PBS) at 4 °C, lumbar spinal cords were transversely sliced and frozen at −80 °C. Ten μm frozen sections were cut using a cryostat. The following primary antibodies were used: monoclonal anti-2′, 3′-cyclic nucleotide-3′-phosphodiesterase (CNPase) for oligodendrocytes (1:1000; Sigma, St. Louis, MO, USA), polyclonal anti-GFAP for astrocytes (1:1000; Dako, Carpinteria, CA, USA), monoclonal OX-42 for microglia/macrophages (1:200; Chemicon, Temecula, CA, USA), and monoclonal OX-6 for activated microglia/macrophages (1:100; Serotec, Raleigh, NC, USA). Horseradish peroxidase-conjugated polymer (Histofine simplestain MAX PO; Nichirei, Tokyo, Japan) was used with secondary antibody for GFAP, OX-42 and OX-6 immunohistochemistry, while the avidin-biotinylated enzyme complex Kit (Vector Laboratories, Burlingame, CA, USA) was used for CNPase immunohistochemistry. Signals were visualized with 3,3-diaminobenzidine substrate kit (Vector Laboratories).

4.3. Reverse transcriptase polymerase chain reaction (RT-PCR) analysis

Cervical spinal cords of wild-type and *mv* rats at 4 and 6 weeks of age were removed and separated into white and gray matter. Total RNA was isolated using SV Total RNA isolation system (Promega, Madison, WI, USA) according to the manufacturer's instructions. One μg of total RNA was transcribed with Superscript II reverse transcriptase using random hexamers (Invitrogen, Carlsbad, CA, USA). To examine gene expression of tumor necrosis factor-α (TNF-α), interleukin-1β (IL-1β), and interleukin-6 (IL-6), first-strand cDNA was amplified by a thermal cycler (PC 707; Astec, Fukuoka, Japan) with GoTaq DNA polymerase (Promega). Details of specific primers are listed in Table 1. β-actin was used as internal standard. To determine relative expression levels of inducible nitric oxide synthase (iNOS) and transforming growth factor-β1 (TGF-β1) gene, SYBR Green-based real-time PCR was performed using LineGene system (BioFlux, Tokyo, Japan). Details of specific primers are listed in Table 1. The cycling condition was as follows: 1 cycle of 95 °C for 1 min, followed by 45 cycles of 95 °C for 15 s, 60 °C for 15 s, and 72 °C for 30 s. The expression ratio relative to β-actin was calculated based on threshold cycle value (Ct).

Table 1 – Primer sets used for RT-PCR analysis

Gene	Primer sequence	Accession number
TNF-α	Sense: 5′-TGTCTACTGAACTTCGGGGTG-3′ Antisense: 5′-GAGGCTGACTTTCTCCTGGTA-3′	X66539
IL-1β	Sense: 5′-AAGCCTCGTGCTGTCGGACCC-3′ Antisense: 5′-TCCAGCTGCAGGGTGGGTGTG-3′	M15131
IL-6	Sense: 5′-ATGAAGTTTCTCTCCGCA-3′ Antisense: 5′-GGGGTAGGAAGGACTATT-3′	M26744
iNOS	Sense: 5′-CCCTAAGAGTCACAAGCATCAA-AAT-3′ Antisense: 5′-GGTTCCTGTTGTTTCTATTTCC-TTTGTTAC-3′	D44591
TGF-β1	Sense: 5'-CTTCAGCTCCACAGAGAAGAAC-TGC-3' Antisense: 5′-CACGATCATGTTGGACAACTG-CTCC-3′	X52498
β-actin	Sense: 5′-TAAAGACCTCTATGCCAACAC-3′ Antisense: 5′-CTCCTGCTTGCTGATCCACAT-3′	BC063166

TNF-α: tumor necrosis factor-α. IL-1β: interleukin-1β. IL-6: interleukin-6. iNOS: inducible nitric oxide synthase. TGF-β1: transforming growth factor-β1.

4.4. Western blot analysis for iNOS protein

Thoracic spinal cords of wild-type and *mv* rats at 10 weeks of age were removed and homogenized in a cell lysis reagent (CelLytic MT; Sigma). After centrifugation at 13,000 rpm for 10 min, protein concentrations were determined by the Bradford Protein Assay (BioRad, Hercules, CA, USA). Ten μg of total proteins in tissue lysates were separated on 7.5% polyacrylamide gels and were electroblotted onto polyvinylidene difluoride membranes (BioRad). Membranes were incubated with monoclonal anti-iNOS antibody as described elsewhere (Nakamura et al., 2006) and monoclonal anti-β-actin antibody (Sigma) at 4 °C overnight and were treated with Histofine simplestain MAX PO for 30 min. Signals were scanned and quantified with a luminescent image analyzer (LAS-3000; Fujifilm, Tokyo, Japan). β-actin was used as internal control.

4.5. In situ hybridization for Atrn mRNA

For riboprobe preparation, a 788-bp fragment of exon 29 of the rat membrane-type *Atrn* (GenBank accession no. AB038387) was amplified by PCR (sense primer, 5′-GGC TCC CAC CTA CCT GTT TAT G-3′, nucleotide position 6454–6475; antisense primer, 5′-TTT GCC TGT TCG TGC TGT G-3′, nucleotide position 7223–7241). The PCR product was subcloned into pGEM T-easy vector (Promega). The *Atrn* cDNA in pGEM plasmid was linearized with SalI or XbaI and digoxigenin (DIG)-labeled RNA probes were synthesized with T7 or SP6 RNA polymerase (Roche Diagnostics, Mannheim, Germany). For *in situ* hybridization, 10 μm frozen sections of the spinal cord were refixed in 4% PFA in PBS for 15 min, rinsed in PBS, and treated with 10 μg/ml proteinase K (Invitrogen) at 37 °C for 12 min, followed by incubation in 4% PFA in PBS for 10 min. After PBS rinse, the sections were treated with 0.2 M HCl for 10 min, rinsed in PBS, and acetylated with 0.2 M triethanolamine (pH 8.0) containing 0.25% acetic anhydride for 10 min. Then they were dehydrated through a graded series of

ethanols and were air-dried for 10 min. DIG-labeled riboprobes were diluted at 1:1000 with hybridization buffer (50% formamide, 10 mM Tris–HCl, pH 8.0, 200 μg/ml yeast tRNA, 10% dextran sulfate, 1× Denhardt's solution, 600 mM NaCl, 0.25% SDS, 1 mM EDTA), denatured at 85 °C for 3 min, and were placed on each slide. The sections were then coverslipped and incubated at 65 °C for 16 h. After hybridization, they were rinsed in 2× sodium saline citrate (SSC) containing 50% formamide at 65 °C for 30 min, treated with 20 μg/ml RNase A (Roche) at 37 °C for 30 min, and rinsed in 2× SSC, 0.2× SSC, and 0.1× SSC (each for 20 min at 65 °C). RNA hybrids were immunostained with alkaline phosphatase-conjugated anti-DIG antibody (Roche) at 4 °C overnight and were visualized using HNPP/Fast Red TR (Roche). For double-labeling by *in situ* hybridization and immunohistochemistry, immunostaining was performed following the *in situ* hybridization color reaction. After rinsing in PBS, the sections were incubated with anti-CNPase or anti-GFAP antibody and reacted with fluorescein isothiocyanate (FITC)-conjugated secondary antibody (Jackson Immunoresearch, West Grove, PA, USA). Signals were detected with a confocal imaging system (C1si; Nikon, Tokyo, Japan) or a digital camera (COOLPIX 4500; Nikon).

4.6. *Cell counts*

The number of CNPase-positive oligodendrocytes was counted in the whole dorsal funiculus of 10-μm transverse sections of the lumbar spinal cord under microscopic observation. Three different fields from three different sections were evaluated. The sections were scanned by a digital camera (Coolpix990; Nikon), and the area of the dorsal funiculus was measured using a software (WinRoof; Mitani Corp., Fukui, Japan). The data are presented as the number of CNPase-positive cells/mm^2.

4.7. *Statistical analysis*

Data are presented as means ± SD. Statistical analysis was performed using one-way analysis of variance followed by Tukey's test or Scheffe's test for immunohistochemistry and RT-PCR analysis and Student's *t* test for Western blot analysis. A value of *P* less than 0.05 was considered statistically significant.

Acknowledgments

We thank Dr. Junji Hirota (Laboratory of Molecular Neuroscience, Osaka Prefecture University) for his technical advice. This work was supported by Grant-in-Aid for Scientific Research from Japan Society for the Promotion of Science (JSPS; nos. 17580268 and 19580359), the Morinaga Foundation for Health and Nutrition, and Kenyuukai (The Veterinary Practitioners Association of Osaka Prefecture University).

REFERENCES

Azouz, A., Gunn, T.M., Duke-Cohan, J.S., 2007. Juvenile-onset loss of lipid-raft domains in attractin-deficient mice. Exp. Cell Res. 313, 761–771.

Bizzozero, O.A., DeJesus, G., Howard, T.A., 2004. Exposure of rat optic nerves to nitric oxide causes protein S-nitrosation and myelin decompaction. Neurochem. Res. 29, 1675–1685.

Boullerne, A.I., Benjamins, J.A., 2006. Nitric oxide synthase expression and nitric oxide toxicity in oligodendrocytes. Antioxid. Redox Signal. 8, 967–980.

Brionne, T.C., Tesseur, I., Masliah, E., Wyss-Coray, T., 2003. Loss of TGF-beta 1 leads to increased neuronal cell death and microgliosis in mouse brain. Neuron 40, 1133–1145.

Delaney, K.H., Kwiecien, J.M., Wegiel, J., Wisniewski, H.M., Percy, D.H., Fletch, A.L., 1995. Familial dysmyelination in a Long Evans rat mutant. Lab. Anim. Sci. 45, 547–553.

Dinulescu, D.M., Fan, W., Boston, B.A., McCall, K., Lamoreux, M.L., Moore, K.J., Montagno, J., Cone, R.D., 1998. *Mahogany* (*mg*) stimulates feeding and increases basal metabolic rate independent of its suppression of agouti. Proc. Natl. Acad. Sci. U. S. A. 95, 12707–12712.

Duke-Cohan, J.S., Morimoto, C., Rocker, J.A., Schlossman, S.F., 1995. A novel form of dipeptidylpeptidase IV found in human serum. J. Biol. Chem. 270, 14107–14114.

Duke-Cohan, J.S., Gu, J., McLaughlin, D.F., Xu, Y., Freeman, G.J., Schlossman, S.F., 1998. Attractin (DPPT-L), a member of the CUB family of cell adhesion and guidance proteins, is secreted by activated human T lymphocytes and modulates immune cell interactions. Proc. Natl. Acad. Sci. U. S. A. 95, 11336–11341.

Duke-Cohan, J.S., Tang, W., Schlossman, S.F., 2000. Attractin: a CUB-family protease involved in T cell-monocyte/macrophage interactions. Adv. Exp. Med. Biol. 477, 173–185.

Duncan, I.D., Lunn, K.F., Holmgren, B., Urba-Holmgren, R., Brignolo-Holmes, L., 1992. The taiep rat: a myelin mutant with an associated oligodendrocyte microtubular defect. J. Neurocytol. 21, 870–884.

Finch, C.E., Laping, N.J., Morgan, T.E., Nichols, N.R., Pasinetti, G.M., 1993. TGF-beta 1 is an organizer of responses to neurodegeneration. J. Cell. Biochem. 53, 314–322.

Gow, A., Friedrich Jr., V.L., Lazzarini, R.A., 1994. Many naturally occurring mutations of myelin proteolipid protein impair its intracellular transport. J. Neurosci. Res. 37, 574–583.

Gunn, T.M., Miller, K.A., He, L., Hyman, R.W., Davis, R.W., Azarani, A., Schlossman, S.F., Duke-Cohan, J.S., Barsh, G.S., 1999. The *mahogany* locus encodes a transmembrane form of human attractin. Nature 398, 152–156.

He, L., Gunn, T.M., Bouley, D.M., Lu, X., Watson, S.J., Schlossman, S.F., Duke-Cohan, J.S., Barsh, G.S., 2001. A biochemical function for attractin in agouti-induced pigmentation and obesity. Nature 27, 40–47.

Herrera-Molina, von Bernhardi, R., 2005. Transforming growth factor-beta 1 produced by hippocampal cells modulates microglial reactivity in culture. Neurobiol. Dis. 19, 229–236.

Hill, K.E., Zollinger, L.V., Watt, H.E., Carlson, N.G., Rose, J.W., 2004. Inducible nitric oxide synthase in chronic active multiple sclerosis plaques: distribution, cellular expression and association with myelin damage. J. Neuroimmunol. 151, 171–179.

Holmgren, B., Urba-Holmgren, R., Riboni, L., Vega-SaenzdeMiera, E.C., 1989. Sprague Dawley rat mutant with tremor, ataxia, tonic immobility episodes, epilepsy and paralysis. Lab. Anim. Sci. 39, 226–228.

Kiefer, R., Schweitzer, T., Jung, S., Toyka, K.V., Hartung, H.P., 1998. Sequential expression of transforming growth factor-beta1 by T-cells, macrophages, and microglia in rat spinal cord during autoimmune inflammation. J. Neuropathol. Exp. Neurol. 57, 385–395.

Knapp, P.E., Skoff, R.P., Redstone, D.W., 1986. Oligodendroglial cell death in jimpy mice: an explanation for the myelin deficit. J. Neurosci. 6, 2813–2822.

Kuramoto, T., Kitada, K., Inui, T., Sasaki, Y., Ito, K., Hase, T., Kawagachi, S., Ogawa, Y., Nakao, K., Barsh, G.S., Nagao, M., Ushijima, T., Serikawa, T., 2001. Attractin/mahogany/zitter

plays a critical role in myelination of the central nervous system. Proc. Natl. Acad. Sci. U. S. A. 98, 559–564.
Kuramoto, T., Nomoto, T., Fujiwara, A., Mizutani, M., Sugimura, T., Ushijima, T., 2002. Insertional mutation of the attractin gene in the black tremor hamster. Mamm. Genome 13, 36–40.
Kuwamura, M., Maeda, M., Kuramoto, T., Kitada, K., Kanehara, T., Moriyama, M., Nakane, Y., Yamate, J., Ushijima, T., Kotani, T., Serikawa, T., 2002. The myelin vacuolation (*mv*) rat with a null mutation in the attractin gene. Lab. Invest. 82, 1279–1286.
Kwiecien, J.M., O'Connor, L.T., Goetz, B.D., Delaney, K.H., Fletch, A.L., Duncan, I.D., 1998. Morphological and morphometric studies of the dysmyelinating mutant, the Long Evans shaker rat. J. Neurocytol. 27, 581–591.
Leon Chavez, B.A., Guevara, J., Galindo, S., Luna, J., Ugarte, A., Villegas, O., Mena, R., Eguibar, J.R., Martinez-Fong, D., 2001. Regional and temporal progression of reactive astrocytosis in the brain of the myelin mutant taiep rat. Brain Res. 900, 152–155.
Leon Chavez, B.A., Aguilar-Alonso, P., Gonzalez-Barrios, J.A., Eguibar, J.R., Ugarte, A., Brambila, E., Ruiz-Arguelles, A., Martinez-Fong, D., 2006. Increased nitric oxide levels and nitric oxide synthase isoform expression in the cerebellum of the taiep rat during its severe demyelination stage. Brain Res. 1121, 221–230.
Lieb, K., Engels, S., Fiebich, B.L., 2003. Inhibition of LPS-induced iNOS and NO synthesis in primary rat microglial cells. Neurochem. Int. 42, 131–137.
Liu, J.S., Zhao, M.L., Brosnan, C.F., Lee, S.C., 2001. Expression of inducible nitric oxide synthase and nitrotyrosine in multiple sclerosis lesions. Am. J. Pathol. 158, 2057–2066.
Lunn, K.F., Clayton, M.K., Duncan, I.D., 1997. The temporal progression of the myelination defect in the taiep rat. J. Neurocytol. 26, 267–281.
Nagle, D.L., McGrail, S.H., Vitale, J., Woolf, E.A., Dussault Jr., B.J., DiRocco, L., Holmgren, L., Montagno, J., Bork, P., Huszar, D., Fairchild-Huntress, V., Ge, P., Keilty, J., Ebeling, C., Baldini, L., Gilchrist, J., Burn, P., Carlson, G.A., Moore, K.J., 1999. The *mahogany* protein is a receptor involved in suppression of obesity. Nature 398, 148–152.
Nakamura, Y., Kitagawa, T., Ihara, H., Kozaki, S., Moriyama, M., Kannan, Y., 2006. Potentiation by high potassium of lipopolysaccharide-induced nitric oxide production from cultured astrocytes. Neurochem. Int. 48, 43–49.
Nunoya, T., Tajima, M., Mizutani, M., Umezawa, H., 1985. A new mutant strain of Syrian hamster with myelin deficiency. Acta. Neuropathol. 65, 305–312.
O'Connor, L.T., Goetz, B.D., Kwiecien, J.M., Delaney, K.H., Fletch, A.L., Duncan, I.D., 1999. Insertion of a retrotransposon in Mbp disrupts mRNA splicing and myelination in a new mutant rat. J. Neurosci. 19, 3404–3413.
O'Connor, L.T., Goetz, B.D., Couve, E., Song, J., Duncan, I.D., 2000. Intracellular distribution of myelin protein gene products is altered in oligodendrocytes of the taiep rat. Mol. Cell. Neurosci. 16, 396–407.
Omlin, F.X., Anders, J.J., 1983. Abnormal cell relationships in jimpy mice: electron microscopic and immunocytochemical findings. J. Neurocytol. 12, 767–784.
Raivich, G., Banati, R., 2004. Brain microglia and blood-derived macrophages: molecular profiles and functional roles in multiple sclerosis and animal models of autoimmune demyelinating disease. Brain Res. Brain Res. Rev. 46, 261–281.
Simons, K., Ikonen, E., 1997. Functional rafts in cell membranes. Nature 387, 569–572.
Simons, M., Kramer, E.M., Thiele, C., Stoffel, W., Trotter, J., 2000. Assembly of myelin by association of proteolipid protein with cholesterol- and galactosylceramide-rich membrane domains. J. Cell. Biol. 151, 143–154.
Skoff, R.P., 1976. Myelin deficit in the jimpy mouse may be due to cellular abnormalities in astroglia. Nature 264, 560–562.
Smith, K.J., Kapoor, R., Felts, P.A., 1999. Demyelination: the role of reactive oxygen and nitrogen species. Brain Pathol. 9, 69–92.
Song, J., O'connor, L.T., Yu, W., Baas, P.W., Duncan, I.D., 1999. Microtubule alterations in cultured taiep rat oligodendrocytes lead to deficits in myelin membrane formation. J. Neurocytol. 28, 671–683.
Tang, W., Gunn, T.M., McLaughlin, D.F., Barsh, G.S., Schlossman, S.F., Duke-Cohan, J.S., 2000. Secreted and membrane attractin result from alternative splicing of the human *ATRN* gene. Proc. Natl. Acad. Sci. U. S. A. 97, 6025–6030.
Tokuda, S., Kuramoto, T., Serikawa, T., 2004. PCR-based genotyping of the rat *Atrn*^{mv} mutation. Exp. Anim. 53, 73–76.
van der Veen, R.C., Roberts, L.J., 1999. Contrasting roles for nitric oxide and peroxynitrite in the peroxidation of myelin lipids. J. Neuroimmunol. 95, 1–7.
Vincent, V.A., Tilders, F.J., Van Dam, A.M., 1997. Inhibition of endotoxin-induced nitric oxide synthase production in microglial cells by the presence of astroglial cells: a role for transforming growth factor beta. Glia 19, 190–198.
Vivien, D., Ali, C., 2006. Transforming growth factor-beta signalling in brain disorders. Cytokine Growth Factor Rev. 17, 121–128.
Vela, J.M., Dalmau, I., Acarin, L., Gonzalez, B., Castellano, B., 1995. Microglial cell reaction in the gray and white matter in spinal cords from jimpy mice. An enzyme histochemical study at the light and electron microscope level. Brain Res. 694, 287–298.
Vela, J.M., Dalmau, I., Gonzalez, B., Castellano, B., 1996. The microglial reaction in spinal cords of jimpy mice is related to apoptotic oligodendrocytes. Brain Res. 712, 134–142.
Zhang, S.C., Goetz, B.D., Carre, J.L., Duncan, I.D., 2001. Reactive microglia in dysmyelination and demyelination. Glia 34, 101–109.
Zhu, Y., Roth-Eichhorn, S., Braun, N., Culmsee, C., Rami, A., Krieglstein, J., 2000. The expression of transforming growth factor-beta1 (TGF-beta1) in hippocampal neurons: a temporary upregulated protein level after transient forebrain ischemia in the rat. Brain Res. 866, 286–298.